Journal of Hazardous Materials 444 (2023) 130410

Contents lists available at ScienceDirect

Journal of Hazardous Materials

journal homepage: www.elsevier.com/locate/jhazmat

$PrsQ_2$, a small periplasmic protein involved in increased uranium resistance in the bacterium *Cupriavidus metallidurans*

Kristel Mijnendonckx [a,1,*], Tom Rogiers [a,1], Francisco J. Giménez del Rey [a,c], Mohamed L. Merroun [d], Adam Williamson [b,2], Md Muntasir Ali [a], Daniel Charlier [c], Natalie Leys [a], Nico Boon [b], Rob Van Houdt [a]

[a] *Microbiology Unit, Interdisciplinary Biosciences, Belgian Nuclear Research Centre, SCK CEN, Mol, Belgium*
[b] *Center for Microbial Ecology and Technology, UGent, Ghent, Belgium*
[c] *Research Group of Microbiology, Department of Bioengineering Sciences, Vrije Universiteit Brussel, Brussels, Belgium*
[d] *Campus Fuentenueva, Department of Microbiology, University of Granada, Granada, Spain*

HIGHLIGHTS

- *Cupriavidus metallidurans* NA4 is able to adapt to toxic uranium concentrations.
- A single mutation increased uranium resistance four times.
- Uranium-phosphate precipitates are formed in the periplasm via an active mechanism.
- We identified the central regulator and essential protein in the adaptive response.

GRAPHICAL ABSTRACT

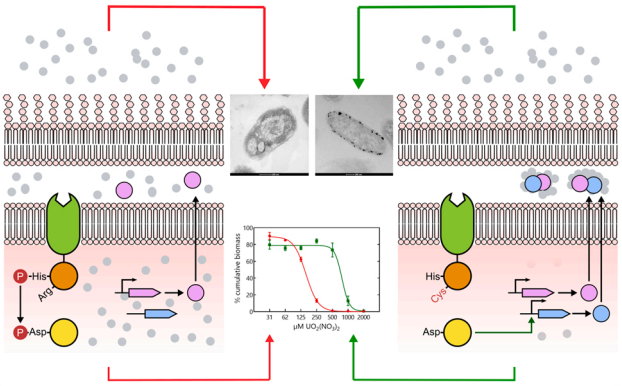

ARTICLE INFO

Keywords:
Cupriavidus metallidurans
Uranium-phosphate precipitation
Two-component system
Adaptation
Regulation

ABSTRACT

Uranium contamination is a widespread problem caused by natural and anthropogenic activities. Although microorganisms thrive in uranium-contaminated environments, little is known about the actual molecular mechanisms mediating uranium resistance. Here, we investigated the resistance mechanisms driving the adaptation of *Cupriavidus metallidurans* NA4 to toxic uranium concentrations. We selected a spontaneous mutant able to grow in the presence of 1 mM uranyl nitrate compared to 250 µM for the parental strain. The increased uranium resistance was acquired via the formation of periplasmic uranium-phosphate precipitates facilitated by the increased expression of a genus-specific small periplasmic protein, $PrsQ_2$, regulated as non-cognate target of

* Correspondence to: Boeretang 200, 2400 Mol, Belgium.
E-mail addresses: kmijnend@sckcen.be (K. Mijnendonckx), rogiers_tom@hotmail.com (T. Rogiers), francisco.javier.gimenez@sckcen.be (F.J. Giménez del Rey), merroun@ugr.es (M.L. Merroun), adjwilliamson@gmail.com (A. Williamson), md.muntasir.ali@sckcen.be (M.M. Ali), dcharlie@vub.be (D. Charlier), natalie.leys@sckcen.be (N. Leys), nico.boon@ugent.be (N. Boon), rob.van.houdt@sckcen.be (R. Van Houdt).
[1] These authors contributed equally to this work
[2] Current address: Centre Etudes Nucléaires de Bordeaux Gradignan, CENBG, Bordeaux, France

https://doi.org/10.1016/j.jhazmat.2022.130410
Received 14 September 2022; Received in revised form 10 November 2022; Accepted 14 November 2022
Available online 15 November 2022

the $CzcS_2$-$CzcR_2$ two-component system. This study shows that bacteria can adapt to toxic uranium concentrations and explicates the complete genetic circuit behind the adaptation.

1. Introduction

Microorganisms are able to survive in extreme environments including radionuclide-contaminated locations imposing a combined chemical and radiological pressure on the microbial community (Simonoff et al., 2007). The most contaminated areas result from nuclear accidents and nuclear weapon testing with Chernobyl, Fukushima or the Nevada test site as well-known examples (Unscear, 1988; Smith et al., 2003; IAEA, 2018). However, contamination is still ongoing due to nuclear industries, but also industries such as mining, geothermal and phosphate industry result in increased concentrations of naturally occurring radionuclide materials (i.e. NORM industries) (IAEA, 2003). One of the principal contaminants of concern is uranium. It is a naturally occurring radionuclide used in industrial activities and it is one of the most important substances of nuclear waste. Environmental contamination of uranium poses a threat when accumulated through the food chain (Reviewed in Ma et al., 2020).

It is well known that microorganisms can influence uranium mobility through biomineralization with phosphates and carbonates, oxidation-reduction reactions, biosorption or uptake and intracellular accumulation (Cologgi et al., 2011; Llorens et al., 2012; Yun et al., 2016; Rogiers, 2022; Yu et al., 2022). However, the underlying molecular mechanisms that entail uranium resistance are largely unknown (Rogiers et al., 2022b). It has been shown that various uranium detoxification mechanisms exist and a single strain can harbor multiple systems (Theodorakopoulos et al., 2015; Yu et al., 2022). Furthermore, depending on the environmental conditions, distinct microbial interactions with uranium are expected to occur. In a reducing environment, uranium reduction is expected to be the dominant mechanism for which cytochromes are shown to be imperative. However, there is currently no model that completely explains the electron transport chain during uranium reduction (You et al., 2021). In oxidizing conditions, uranium resistance is mostly attributed to phosphatases forming needle-like uranyl precipitates at different cellular localizations (Yung and Jiao, 2014; Khare et al., 2020; Pinel-Cabello et al., 2021). Siderophores have been shown to form stable complexes with metals and some radionuclides, thus they could be important to protect cells from uranium stress through sequestration (Rajkumar et al., 2010). Recently, a single pass transmembrane protein, UipA, has been identified as a key protein in uranium resistant strains. Although its precise role is not yet explicated, its affinity for both uranium and iron suggest a link between iron and uranium metabolism (Gallois et al., 2021). Next to precipitation, uranium efflux has been shown to contribute to uranium resistance (Theodorakopoulos et al., 2015; Khare et al., 2020). Nevertheless, no dedicated uranium efflux system has been identified to date. Putatively the outer membrane transporter Rsa_F of *Caulabactor cresentus* is involved in uranium efflux but a role in maintaining outer membrane integrity cannot be excluded (Yung et al., 2015). Understanding the detailed molecular mechanisms is important to correctly assess the impact microbes exert on the mobility of uranium. Furthermore, it can aid in exploiting bioremediation techniques. Investigating the adaptation potential of bacteria to uranium further provides details on uranium resistance mechanisms.

Recently, we showed that *Cupriavidus metallidurans* NA4 precipitates uranium from growth medium as uranium phosphate complexes that are associated with polyhydroxybutyrate (Rogiers et al., 2022a). *C. metallidurans* is a model organism for metal resistance and strains are usually isolated from industrially metal-contaminated sites (Mergeay and Van Houdt, 2015; Bobe et al., 2008). *C. metallidurans* species contain numerous mobile genetic elements allowing rapid adaptation to toxic circumstances (Mijnendonckx et al., 2011; Van Houdt et al., 2018). The adaptation potential of *C. metallidurans* NA4 has also previously been shown for silver and platinum (Ali et al., 2019; Mijnendonckx et al., 2019). Here, we investigate the adaptation potential of *C. metallidurans* NA4 to toxic uranium concentrations and explicate the genetic circuit behind the increased uranium resistance.

2. Materials & methods

2.1. Strains and growth conditions

The list of strains used in this study is presented in Table 1. *C. metallidurans* strains were routinely cultured in RM medium (Mergeay et al., 1985) supplemented with 0.2% (w/v) sodium gluconate as a carbon source at 30 °C with shaking at 120 rpm. For culturing on solid media, 2% agar (bacteriological, OXOID, United Kingdom) was added or 1.5% noble agar (MERCK NV, Belgium) when supplemented with metal salts. Metal salts used in this study included $UO_2(NO_3)_2.6\ H_2O$ (dissolved in 100 mM HCl, SPI chemicals, USA), $CdCl_20.2.5\ H_2O$ (Alfa Aesar, USA), $CuCl_20.2\ H_2O$, $NiCl_20.6\ H_2O$, $Pb(NO_3)_2$, $CoCl_20.6\ H_2O$, $AgNO_3$ (MERCK NV, Belgium) and $ZnCl_2$. *Escherichia coli* strains were routinely cultured in LB medium at 37 °C. When appropriate, the following antibiotics were added to the growth medium at the indicated final concentrations: kanamycin sulfate (50 μg mL^{-1} for *E. coli* or 1500 μg mL^{-1} for *C. metallidurans*) (Km^{50}; Km^{1500}), tetracycline hydrochloride (20 μg mL^{-1}) (Tc^{20}) and trimethoprim (100 μg mL^{-1}) (Tm^{100}).

2.2. Generation of the spontaneous uranium resistant mutant

The spontaneous uranium resistant mutant *C. metallidurans* NA4U was obtained by exposing *C. metallidurans* NA4 to a toxic uranium concentration. To this end, a stationary phase culture of *C. metallidurans* NA4 was diluted 100 times in liquid RM medium supplemented with 400 μM $UO_2(NO_3)_2{\bullet}6\ H_2O$. When growth was observed after one week, the culture was plated on non-selective RM agar medium. Finally, purified colonies were screened for uranium resistance.

2.3. Metal resistance

Metal resistance was analyzed by a spotting assay. To this end, a ten-fold dilution series from 10^0 until 10^{-7} was prepared from three independent stationary phase cultures with 10^9 cells/mL. The dilution series was spotted (10 μL) on RM noble agar plates supplemented with/without 7.5 mM $CoCl_2$, 20 mM $NiCl_2$, 1 mM $CdCl_2$, 6 mM $ZnCl_2$, 0.5 mM $CuCl_2$ or 500 μM $UO_2(NO_3)_2$. Resistance to silver was scored on LB agar plates supplemented with 0.5 mM $AgNO_3$. Spots were counted after four days at 30 °C. The % log survival was calculated by dividing the log (cells/mL) of the agar plates with metal salts by the log(cells/mL) of the agar plates without metal salts.

In addition, three independent stationary phase cultures grown in RM medium for two days were pelleted for 5 min at 8 500 g, washed with 10 mM $MgSO_4$ and diluted to a cell concentration of 10^7 cells/mL in a flat bottom 96-well plate (Cellstar 96 Well Cell Culture Plate, Greiner Bio- One, Belgium) that contained RM medium with or without different $UO_2(NO_3)_2$ concentrations. Growth was assessed by monitoring OD_{595} for three days at 30 °C, 300 rpm continuous shaking in a 96-well plate reader (Multiskan Ascent, Thermo Labsystems, USA). Growth curves were analyzed with the R Growthcurver package (version 0.3.1) (Sprouffske and Wagner, 2016; R Core Team, 2017) by dividing the empirical area under curve (auc_e) in the presence of uranium by the auc_e in the absence of uranium.

Table 1
Strains and plasmid used in this study.

Strains	Genotype/relevant characteristics	Ref.
Escherichia coli		
DG1	*mcrA* Δ*mrr-hsdRMS-mcrBC* (r_Bm_B) Φ80*lacZ*Δ*M15* Δ*lacX74 recA1 araD139* Δ(*ara-leu*)*7697 galU galK rpsL endA1 nupG*	Eurogentec, Belgium
MFD*pir*	MG1655 RP4–2-Tc::[Δ*Mu1*::*aac(3)IV*-Δ*aphA*-Δ*nic35*-Δ*Mu2*::*zeo*] Δ*dapA*::*(erm-pir)* Δ*recA*	(33)
SoluBL21	F- *ompT hsdSB* (r_B- m_B-) *gal dcm* (DE3)	Genlantis, USA
TOP10	F- *mcr*A Δ(*mrr-hsd*RMS-*mcr*BC) Φ80*lacZ*Δ*M15* Δ*lacX74 rec*A1 *ara*D139 Δ(*araleu*)7697 *gal*U *gal*K *rps*L (StrR) *end*A1 *nup*G	Invitrogen, Belgium
Cupriavidus metallidurans		
NA4	Isolated from ISS SRV-K filter reactor effluent returned on Soyuz 10S (2004) (original code: 0502478–1)	(23)
NA4U	Spontaneous uranium mutant of NA4, U^R	This study
NA4Δ*czcS2*^{Tc}	*czcS*$_2$::*tet*, TcR	This study
NA4Δ*czcS2*^{Tm}	*czcS*$_2$::*dfr*, Tm^R	This study
NA4UΔ*czcR*$_2$*S*$_2$	*czcR*$_2$*S*$_2$::*km*, Km^R	This study
NA4UΔ*phoA*$_1$*A*$_2$	*phoA*$_1$*A*$_2$::*dfr*, TmR	This study
NA4UΔ*prsQ*$_2$	*prsQ*$_2$::*dfr*, Tm^R	This study
Plasmids	Genotype/relevant characteristics	Ref.
pACYC177	p15A ori, Amp^R, Km^R	Lab collection
pACYC184	p15A ori, Cm^R, Tc^R	Lab collection
pBBR1MCS-2	pBBR1 ori, Mob^+, *lacZ*, Km^R	(31)
pBBR1MCS2-*dfr*	pBBR1 ori, Mob^+, *lacZ*, Km^R, Tm^R	Lab collection
pBBR-*prsQ*$_2$	*prsQ*$_2$of NA4 in pBBR1MCS-2, Km^R	(26)
pET-*czcR*$_2$	CDS of *czcR*$_2$ from NA4 in pET24a(+), Km^R	This study
pET-*czcR*$_2^{D51A}$	pET24-*czcR*$_2$ with D51A substitution in $CzcR_2$, Km^R	This study
pK18mob	pMB1 ori, Mob^+, *lacZ*, Km^R	(32)
pK18mob_*tet*	pMB1 ori, Mob^+, *lacZ*, Tc^R	Lab collection
pK18mob-*czcR*$_2$*S*$_2$	pK18mob with *czcR*$_2$*S*$_2$ gene region of NA4, Km^R	This study
pK18mob-*czcS*$_2$::*dfr*	pK18mob-*czcR*$_2$*S*$_2$ derivative with *czcS*$_2$ replaced by *dfr*, Km^R, Tm^R	This study
pK18mob-*czcS*$_2$::*tet*	pK18mob-*czcR*$_2$*S*$_2$ derivative with *czcS*$_2$ replaced by *tet*, Km^R, Tc^R	This study
pK18mob-*phoA*$_1$*A*$_2$	pK18mob with *phoA*$_1$*A*$_2$ gene region of NA4, Km^R	This study
pK18mob-*phoA*$_1$*A*$_2$::*dfr*	pK18mob- *phoA*$_1$*A*$_2$ derivative with *phoA*$_1$*A*$_2$ replaced by *dfr*, Km^R, Tm^R	This study
pK18mob-*prsQ*$_2$	pK18mob with *prsQ*$_2$ gene region of NA4, Km^R	(26)
pBBR-*prsQ*$_2^{SDM}$	pBBR-*prsQ*$_2$ harbouring a frameshift in the start codon of *prsQ*$_2$, Km^R	(26)
pBBR-*prsQ*$_2^{\Delta SP}$	pBBR-*prsQ*$_2$ with 26-bp deletion of the *prsQ*$_2$ signal sequence, Km^R	(26)
pK18mob-*prsQ*$_2$::*dfr*	pK18mob-*prsQ*$_2$derivative with *prsQ*$_2$ replaced by *dfr*, Km^R, Tm^R	This study
pSCK201-*czcR*$_2$*S*$_2$	pSCK201 with *czcR*$_2$*S*$_2$ gene region of NA4, Tm^R	This study
pSCK201-*czcR*$_2$*S*$_2$::*km*	pSCK201-*czcR*$_2$*S*$_2$derivative with *czcR*$_2$*S*$_2$ replaced by *km*, Tm^R, Km^R	This study

U^R (uranium resistant); Km^R and *km* (kanamycin resistance and resistance gene); Tc^R and *tet* (tetracycline resistance and resistance gene); Tm^R and *dfr* (trimethoprim resistant and resistance gene)

2.4. Interaction of C. metallidurans NA4U with uranium

Growth of *C. metallidurans* NA4U was followed for 24 h in the presence of 0 μM, 100 μM and 250 μM $UO_2(NO_3)_2$. Detailed protocols are described in Supplementary Information.

2.5. Transmission electron microscopy

Microscopic analysis was performed after 24 h growth in presence of either 100 μM or 250 μM $UO_2(NO_3)_2$. The detailed procedure is described in Supplementary Information.

2.6. Construction of insertional inactivation constructs

Phusion High-Fidelity Polymerase (Thermofisher Scientific, Belgium) was routinely used for the amplification of DNA. Anza restriction enzymes and T4 ligase (Thermofisher Scientific, Belgium) or the GeneArt™ seamless cloning and assembly enzyme mix (GA cloning, Thermofisher Scientific, Belgium) were used for cloning purposes. Plasmids and primers used in this study are shown in Table 1 and Supplementary Table 1 respectively. The tetracycline resistance cassette was amplified from pACYC184 with primers Ampli.*tet*-5 and Ampli.*tet*-3 (1.3 kb) for GA cloning or with primers *tet*_FW and *tet*_RV (1.4 kb) for digestion with *Bcu*I and *Bsp*TI. Antibiotic resistance genes *dfr* (trimethoprim resistance, Tm^R) and *km* (kanamycin resistance, Km^R) were amplified from pBBR1MCS2-*dfr* (originally derived from Kovach et al. (1995) and pACYC177 with primers *dfr*_5'_*Bcu*I and *dfr*_3'_*Bsp*TI (0.4 kb), and KmFOR-*Bcu*I and Km_REV_*Bsp*TI (1.0 kb), respectively. Amplicons of *dfr* and *km* were afterwards digested with *Bcu*I and *Bsp*TI for ligation with digested inverse PCRs. All intermediate and final constructs were transformed to either *E. coli* DG1 (Eurogentec, Belgium) or TOP10 (Invitrogen, Belgium) chemically competent cells.

Primer pair *prsQ*$_2$_*Xba*I and *czcS*$_2$_*Hin*dIII was used to amplify the *C. metallidurans* NA4 gene region of *czcR*$_2$*S*$_2$ including 2.5 kb upstream and 0.6 kb downstream providing an amplicon with a size of 5.3 kb and *Xba*I and *Hin*dIII restriction sites. The amplified region was cloned in pK18mob (Schafer et al., 1994) linearized with *Xba*I and *Hin*dIII. The resulting plasmid, pK18mob-*czcR*$_2$*S*$_2$, was used as PCR template with outward-oriented primer pair *czcR*$_2$*S*$_2$_inverse_3′ and *czcS*$_2$_inverse_5′ (5.7 kb). Amplified product was digested with *Bcu*I and *Bsp*TI and ligated with either *Bcu*I/*Bsp*TI digested *tet* or *dfr* to create pK18mob-*czcS*$_2$::*tet* and pK18mob-*czcS*$_2$::*dfr*, respectively. Plasmid pK18mob-*czcR*$_2$*S*$_2$ was also used as template for the primer pair *czcS*$_2$_Rv_*Hin*dIII and pK18mobInverse_GA_RV (4.2 kb). The amplicon was cloned in pSCK201, which was linearized with *Hin*dIII and *Sac*I resulting in the construct pSCK201-*czcR*$_2$*S*$_2$. This plasmid was then used as template for inverse PCR with primers *czcR*$_2$*S*$_2$_inverse_5' and *czcR*$_2$*S*$_2$_inverse_3' (3.9 kb). The amplified product was *Bsp*TI/*Bcu*I digested and ligated with the digested *km*, creating pSCK201-*czcR*$_2$*S*$_2$::*km*.

The CmetNA4_v1_pA0288 and CmetNA4_v1_pA0287 (hereafter *phoA*$_1$ and *phoA*$_2$) gene region with 0.8 kb upstream and 0.5 kb downstream was amplified with primers *phoA1*_FW_*Eco*RI and *phoA2*_RV_*Bam*HI, resulting in an amplicon of 4.2 kb with *Eco*RI and *Bam*HI restriction sites. This was cloned into *Eco*RI and *Bam*HI restricted pK18mob and the resulting plasmid, pK18mob_*phoA*$_1$*A*$_2$, was transformed to *E. coli* DG1. Inverse PCR was performed on pK18mob_*phoA*$_1$*A*$_2$with primers *phoA1*_5'_inverse_*Bcu*I and *phoA2*_3'_inverse_*Bsp*TI, the resulted amplicon was restricted with *Bcu*I and *Bsp*TI and the *dfr* trimethoprim resistance gene was cloned as a *Bcu*I/*Bsp*TI fragment in the inverse amplified pK18mob_*phoA*$_1$*A*$_2$, resulting in pK18mob_*phoA*$_1$*A*$_2$::*dfr*. The *prsQ*$_2$ gene region was amplified with *prsQ*$_2$_5′_FW and *prsQ*$_2$_3′_RV, followed by GA cloning with pK18mob_GA_Fw/pK18mob_GA_Rv amplified pK18mob resulting in the construct pK18mob_*prsQ*$_2$. This was used as template for inverse PCR was performed with primers *prsQ*$_2$-BspTI-INV-5′ and *prsQ*$_2$_RV (6.6 kb). The amplified product was *Bsp*TI/*Bcu*I digested and ligated with digested *dfr* to obtain the pK18mob-*prsQ*$_2$::*dfr* construct.

All created plasmids were confirmed by Sanger sequencing with outward oriented antibiotic resistance gene primers: *tet*-5_out and *tet*-3_out, *dfr*out_5′ and *dfr*out_3′, and Rev_*Km*_upstream and Rev_*Km*_downstream.

For insertion mutagenesis, all constructs were conjugated in *C. metallidurans* NA4U or NA4 (for pK18mob-*czcS*$_2$::*tet* and pK18mob-*czcS*$_2$::*dfr*) via *E. coli* MFD*pir* as donor (biparental) (Ferrieres et al., 2010). For each mutant, a trimethoprim resistant and kanamycin sensitive exconjugant was selected (kanamycin resistant and tetracycline sensitive in the case of *czcR*$_2$*S*$_2$::*km* and a tetracycline resistant and kanamycin sensitive in the case of *czcS*$_2$::*tet*) yielding NA4Δ*czcS*$_2^{Tc}$,

NA4Δ*czcS*$_2$™, NA4UΔ*czcR*$_2$*S*$_2$, NA4UΔ*phoA*$_1$*A*$_2$and NA4UΔ*prsQ*$_2$.

Furthermore, plasmids pBBR1MCS-2, pBBR-*prsQ*$_2$, pBBR-*prsQ*$_2^{SDM}$ pBBR-*prsQ*$_2^{\Delta SP}$ (Mijnendonckx et al., 2019) were transformed by electroporation in NA4UΔ*prsQ*$_2$.

2.7. Construction of plasmids for heterologous expression

The CDS of *czcR*$_2$ was amplified by PCR using genomic DNA from *C. metallidurans* NA4 as template with the *czcR*$_2$_FW-RV primer pair. The PCR product was cloned as *Nde*I/*Xho*I fragments into pET24a(+). The resulting pET24-*czcR*$_2$ plasmid from *E. coli* DG1 transformants selected on LB Km50 were further confirmed by sequencing with the primers T7_FW and T7_term. Subsequently, pET24-*czcR*$_2$ were transformed by electroporation into *E. coli* SoluBL21. In addition, a D51A mutation was introduced into pET24-*czcR*$_2$ via site-directed mutagenesis (Phusion Site-Directed Mutagenesis Kit, Thermo Scientific, Belgium). Briefly, plasmid pET24-*czcR*$_2$ was used as template for PCR amplification with the phosphorylated primer pairs *czcR*$_2$_D51A_FW/ *czcR*$_2$_SDM_RV. The resulting linear fragment was purified using the Wizard® SV Gel and PCR Clean-Up System (Promega, the Netherlands), *Dpn*I treated, self-ligated and transformed to *E. coli* DG1. The resulting pET24-*czcR*$_2^{D51A}$ plasmid from transformants selected on LB Km50 were further confirmed by sequencing prior to transformation into *E. coli* SoluBL21.

2.8. Whole genome sequencing

Total genomic DNA of *C. metallidurans* NA4U and NA4Δ*czcS*$_2^{Tc}$ was extracted from liquid cultures using the QIAamp DNA Mini Kit (Qiagen Benelux, Belgium). Dropsense Lunatic chips (Unchained Labs, Belgium) were used to analyze the quantity and quality of the extracted DNA. Whole genome sequencing was performed with the Illumina MiSeq platform at Baseclear (Leiden, The Netherlands), paired-end sequencing reads were analyzed by alignment to the reference genome of NA4 using breseq version 0.25.0 (Heath et al., 2014).

2.9. Whole genome expression analysis

Gene expression in the spontaneous uranium mutant NA4U and in the insertional deletion mutant NA4Δ*czcS*$_2^{Tc}$ was compared to that of the parental strain in non-selective conditions. First, three independent cultures were grown until stationary and diluted 1/500. Then, subcultures were incubated at 120 rpm 30 °C and the OD_{600} was followed until 0.6. Hereafter, subcultures were centrifuged for 5 min at 12 000 g in 2 mL portions. The supernatant was discarded and pellets were snap frozen in liquid nitrogen before storage in − 80 °C.

RNA was extracted from the pellets using the Promega SV total RNA isolation system (Promega, USA). RNA sequencing (directional mRNA library, RiboZero rRNA depletion and 2 × 125 bp paired-end sequencing) was performed by Eurofins Genomics GmbH (Ebersberg, Germany). RNA of NA4Δ*czcS*$_2^{Tc}$ and corresponding parental strain were extracted from the pellets using the *mir*Vana™ miRNA isolation kit (Invitrogen™, USA) with the protocol for total RNA extraction. RNA sequencing was performed by Vertis Biotechnologie AG (Freising, Germany). The RNA-seq datasets generated and analyzed for this study are available from the NCBI Sequence Read Archive under accession number PRJNA849803. Read alignment to the *C. metallidurans* NA4 genome (v2 MaGe platform (Vallenet et al., 2013) and strand-specific read counting (featureCounts) were done with the Rsubread package for R (Liao et al., 2019). Differential gene expression of the resulting count matrix was accomplished using edgeR (Robinson et al., 2009) and limma (Ritchie et al., 2015), using a Benjamini–Hochberg approach to control for Type 1 statistical errors. Genes were found to be differentially expressed if they showed a $\log_2$ fold change higher than 1 or lower than − 1 and a p-value value lower than 0.05. Further analysis was performed based on the eggNOG functional classification (Powell et al., 2012), downloaded from the MaGe platform (Vallenet et al., 2013), and p-values for classes with known function were calculated using the R MLP package (version 1.34.0) (Raghavan et al., 2019).

2.10. Protein expression and purification of 6xHis-tagged proteins

E. coli SoluBL21 containing pET24-*czcR*$_2$ or pET24-*czcR*$_{2D51A}$ was cultured overnight at 37 °C and diluted 1:500 in 2 L LB broth containing 50 μg/mL kanamycin. Cells were grown aerobically with vigorous shaking (180 rpm) at 37 °C to an OD_{600} of 0.6–0.8. Next, IPTG was added at a final concentration of 0.3 mM to induce protein expression. After overnight induction at 20 °C (180 rpm), cells were harvested by centrifugation (5000 g, 20 min at 4 °C) prior to lysis by sonication. Sonication and recovery were carried out in a lysis buffer (50 mM Tris-HCl, 100 mM NaCl, 5% glycerol, pH 7.5) supplemented with 1 mM PMSF (phenylmethylsulfonyl fluoride) and 1 mM benzamidine. The cell lysate was clarified by centrifugation (13 000 g, 45 min at 4 °C), loaded onto a HisTrap HP column (GE Lifesciences) in binding buffer (50 mM Tris-HCl, 100 mM NaCl, 30 mM imidazole, 5% glycerol, pH 7.5) and eluted with the same buffer supplemented with 500 mM imidazole. The proteins were subsequently purified by size-exclusion chromatography (SEC) on a HiLoad 16/600 Superdex 75 pg (16 mm x 600 mm) (GE Lifesciences). The purity of all protein preparations was determined by SDS-PAGE and protein concentrations measured with the Bradford protein assay (BioRad) using BSA (bovine serum albumin) as a standard. All protein concentrations are expressed in monomer equivalents.

2.11. Electrophoretic mobility shift assays

Single 5′-end radiolabeled [5′-^{32}P] DNA fragments were prepared by PCR amplification with GoTaq green master mix (Promega), genomic DNA from *C. metallidurans* NA4 and the CzcR$_2$_EMSA_FW/RV or the v2_1370_FW/RV primer pair (Supplementary Table 1), one primer was [5′-^{32}P] end labelled with [γ-^{32}P]-ATP (3000 Ci/mmol; Perkin-Elmer) using T4 polynucleotide kinase (Fermentas) as described in (Nguyen Ple et al., 2010). EMSAs were performed according to Enoru-Eta et al. (Enoru-Eta et al., 2000) and in the presence of excess of non-specific, non-labelled competitor DNA (25 μg/mL sonicated herring sperm DNA). Complex formation was performed at RT (room temperature) and allowed to reach equilibrium for 30 min in phosphate binding buffer (25 mM Na_2HPO_4, 150 mM NaCl, 0.1 mM EDTA, 2 mM $MgCl_2$, 1 mM DTT, 10% glycerol, pH 7.0). Protein-DNA complexes were separated from unbound DNA by gel electrophoresis on 6% polyacrylamide with TBE buffer (89 mM Tris-base, 89 mM boric acid, 2.5 mM EDTA) as running buffer.

3. Results

3.1. Selection of increased uranium resistance

Although growth of *C. metallidurans* NA4 was not observed in liquid RM medium supplemented with 400 μM $UO_2(NO_3)_2$ after a standard three-day growth assay, growth was visible after extended incubation (1 week). The culture was streaked on non-selective RM agar and retested for its resistance. The latter, designated as NA4U, exhibited an increased and inheritable resistance to uranium. Growth of NA4U in the presence of uranium was only slightly hampered up to 500 μM and completely inhibited at 2 mM, while the parental NA4 strain showed growth impairment from 125 μM onwards and complete inhibition between 250 and 500 μM (Fig. 1a). In non-selective conditions, no growth differences were observed between both strains (Supplementary Fig. 1). In addition, NA4U exhibited decreased resistance towards Co^{2+} and Ni^{2+}, and increased resistance to Cd^{2+}, Zn^{2+}, Cu^{2+} and Ag^{+} (Fig. 1b).

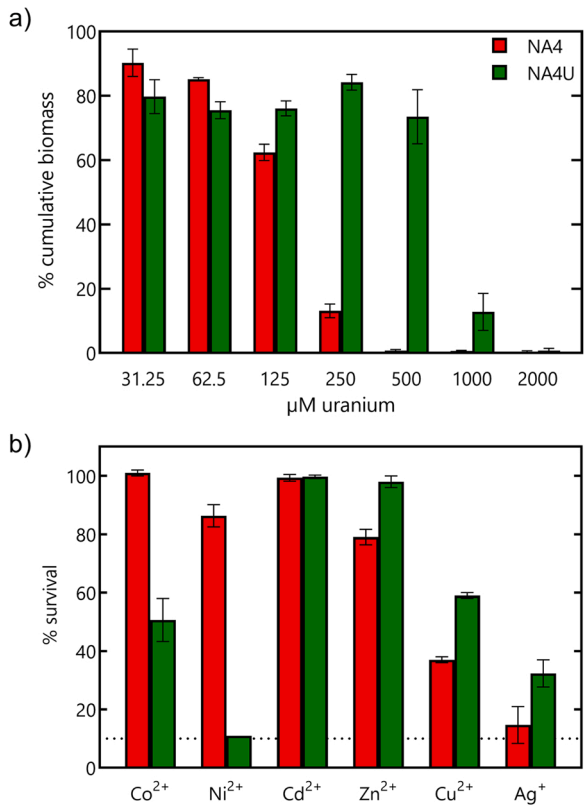

Fig. 1. Growth of *C. metallidurans* strains in different conditions. (a) Growth of *C. metallidurans* strains NA4 (red) and NA4U (green) in RM medium supplemented with different uranium concentrations. Data (average and standard deviation) is shown as the percentage of cumulative biomass based on the empirical area under curve after 72 h. (b) Comparison of metal resistance to 7.5 mM Co^{2+}, 20 mM Ni^{2+}, 1 mM Cd^{2+}, 6 mM Zn^{2+}, 0.5 mM Cu^{2+} and 0.5 mM Ag^{+}. Data (average and standard deviation) is presented as % survival. The detection limit is presented as a dotted line. All assays consist of three biological replicates.

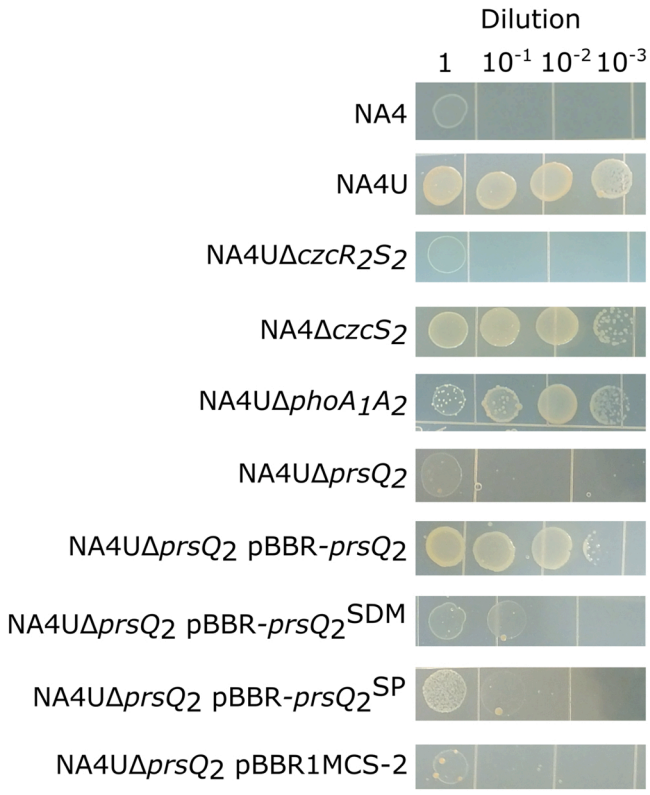

Fig. 2. Growth of different *C. metallidurans* insertional knockout mutants on uranium. Tenfold serial dilution of a stationary phase cultures spotted on RM agar supplemented with 500 µM $UO_2(NO_3)_2$ and incubated for four days at 30 °C. The results are shown for one representative of three independent cultures of NA4, NA4U, and all insertional knockout mutants (preceding Δ) and complementation strains (designated with pBBR). pBBR-$prsQ_2^{SDM}$ complementation of $prsQ_2$ with a frameshift mutation in the start codon; pBBR-$prsQ_2^{\Delta SP}$: complementation of $prsQ_2$ without signal peptide.

3.2. Regulation of increased uranium resistance by the response regulator *CzcR₂*

Whole genome sequencing of NA4U revealed several single nucleotide polymorphisms (SNPs) and indels (Supplementary Table 2). The largest deletion consisted of 55 consecutive genes (CmetNA4_v2_2332 – 2386) belonging to a putative prophage (Van Houdt et al., 2018). In addition, *czcS₂* (1446 bp), coding for a sensor histidine kinase, was inactivated due to a large 999-bp deletion. The latter resulted in the overexpression of *czcR₂*, encoding the response regulator of the two-component system (TCS) $CzcR_2S_2$, as evidenced by comparing the NA4U transcriptome to that of the parental strain in non-selective growth conditions (Supplementary Table 3). The NA4U transcriptome showed, with 587 up- and 416 downregulated genes, many changes but none of the other NA4U genes affected by SNPs and/or indels were differentially expressed (Supplementary Tables 2 and 3). The TCS $CzcR_2S_2$, which is located on the chromid (CmetNA4_v1_pm0619-pm0620), regulates the efflux pump $CzcC_2B_2A_2$ (CmetNA4_v1_pm0612-pm0614) involved in cadmium, zinc and cobalt resistance (Nies et al., 1987; Diels et al., 1995). However, both *C. metallidurans* NA4 and NA4U have a 2-bp deletion in *czcC₂* resulting in a premature stop codon (Rogiers et al., 2022a). Combined with a comparable expression level of *czcA₂* in NA4 and NA4U (Supplementary Table 3), the $CzcC_2B_2A_2$ pump is not considered as instigator for the increased uranium resistance. Nevertheless, deletion of *czcR₂S₂* in NA4U decreased uranium resistance to that of NA4 and deletion of *czcS₂* in NA4 increased uranium resistance to that of NA4U (Fig. 2, Supplementary Fig. 2), corroborating a role for $CzcR_2$ in the acquired increased uranium resistance. In addition, the resistance level of NA4Δ*czcS₂* to Ni^{2+}, Co^{2+}, Cd^{2+}, Zn^{2+} and Cu^{2+} was not comparable to that of NA4U, indicating that these metal resistance determinants do not play a role in the increased uranium resistance. Only resistance to Ag^{+} of NA4Δ*czcS₂* was comparable to that of NA4U and not NA4 (Supplementary Fig. 3).

3.3. A key role for the small periplasmic protein *PrsQ₂*

Next, possible target genes of $CzcR_2$ resulting in the increased uranium resistance were identified by comparing the transcriptome of NA4U and NA4Δ*czcS₂* to NA4 in non-selective conditions. The latter revealed 62 and 10 genes that were commonly upregulated and downregulated, respectively. Noteworthy, in contrast to strain NA4U, for which the transcriptomic landscape in non-selective conditions strongly differed from that of NA4, only 86 and 201 genes were up- and downregulated in non-selective growth conditions in strain NA4Δ*czcS₂* compared to NA4 (Supplementary Fig. 4, Supplementary Table 3). On scrutinizing the list of commonly upregulated genes, two genes attracted attention, namely, *phoA₁* encoding an alkaline phosphatase and *prsQ₂* encoding a small periplasmic protein. Phosphatases have been shown to be involved in the precipitation of uranium in many strains (Beazley et al., 2007; Kulkarni et al., 2013; Macaskie et al., 2000; Nilgiriwala et al., 2008; Pinel-Cabello et al., 2021; Powers et al., 2002; Yung and Jiao, 2014). However, deletion of the *phoA₁A₂* operon in NA4U did not affect uranium resistance (Fig. 2). The *prsQ₂* gene was one of the highest commonly upregulated genes in NA4U and NA4Δ*czcS₂* (Supplementary

Table 3) and was previously shown to be involved in increased silver resistance (Mijnendonckx et al., 2019), which was also observed in NA4U and NA4Δ*czcS*$_2$. Unlike the deletion of *phoA*$_1$, deletion of *prsQ*$_2$ decreased uranium resistance to the parental level, which could be restored to that of NA4U by plasmid-based complementation of the full-length *prsQ*$_2$ (Fig. 2). Furthermore, CzcR$_2$ binding to the *prsQ*$_2$ promoter was confirmed by EMSA (Fig. 3). The latter also indicated that binding of dephosphomimetic CzcR$_2^{D51A}$, reflecting the phosphorylation state of CzcR$_2$ in the absence of CzcS$_2$ (i.e. in NA4U and NA4Δ*czcS*$_2$) occurred with higher affinity than binding of CzcR$_2$ (Fig. 3).

3.4. NA4U actively removes uranium but with a different subcellular localization at a higher concentration

Next, we investigated the removal of uranium by strain NA4U in the presence of 100 and 250 μM $UO_2(NO_3)_2$. After 24 h NA4U removed 96.7 ± 0.3% and 98.2 ± 0.0% of 100 and 250 μM uranium, respectively (Fig. 4a). When CCCP, a chemical known to inhibit the proton motive force (Ikonomidis et al., 2008), was added to metabolically inactivate the cells, uranium removal was not observed (Fig. 4a). It should be noted that addition of CCCP also affected the total cell number, which increased gradually in the presence of 100 and 250 μM $UO_2(NO_3)_2$, but remained constant for the CCCP-treated controls (Fig. 4b).

To visualize possible uranium precipitates, TEM analysis was performed after 24 h of growth of NA4U in the presence of 100 μM $UO_2(NO_3)_2$. Similar to the parental strain, intracellular uranium precipitates were observed (Supplementary Fig. 5) (Rogiers et al., 2022a). However, when the uranium concentration was increased to 250 μM, uranium-phosphate precipitates were formed in NA4U as well as NA4Δ*czcS*$_2$ that were mainly in the periplasm (Fig. 5, Supplementary Fig. 6). Noteworthy, as growth of the parental strain at 250 μM $UO_2(NO_3)_2$ was limited, no TEM pictures could be obtained.

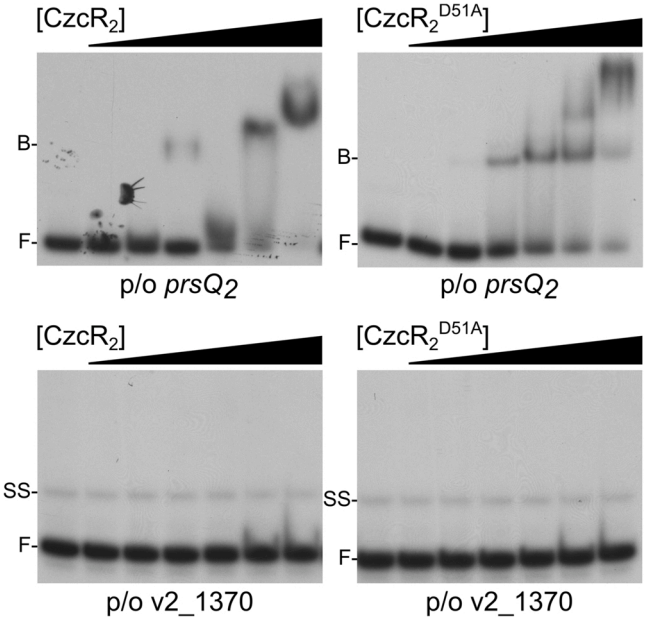

Fig. 3. Electrophoretic mobility shift assays. EMSA corresponding to the binding of CzcR$_2$-6xHis and CzcR$_2^{D51A}$-6xHis with the control region of *prsQ*$_2$ (upper panel) and v2_1370 (lower panel). The latter was used as a negative control. Protein concentrations (expressed in monomer equivalents) extended from 3.13 μM to 50 μM with a stepwise two-fold increase. The small vertical line indicates no protein. The position of free DNA (F) and protein-DNA complexes (B) are indicated.

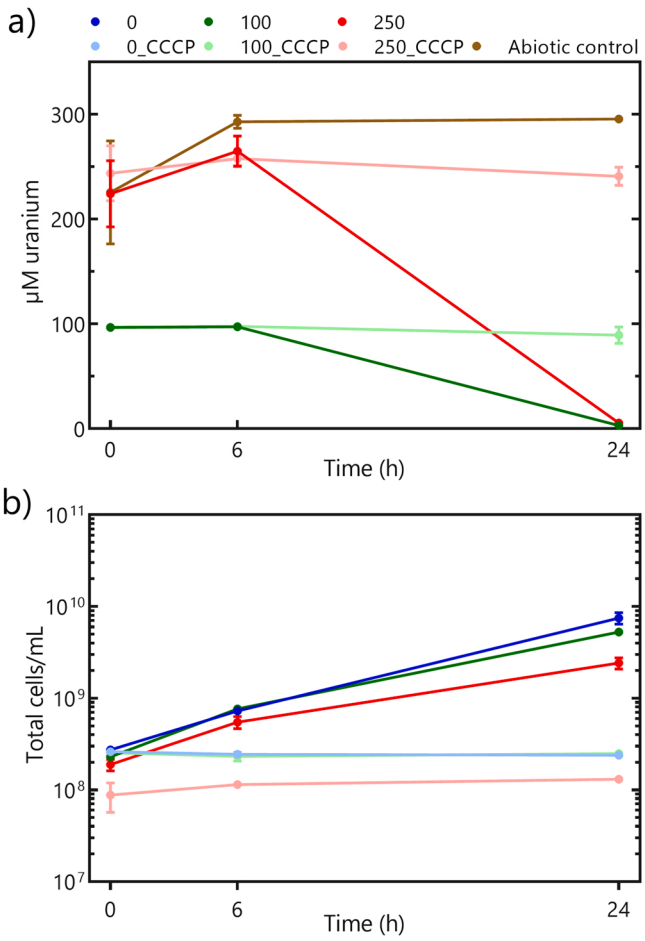

Fig. 4. Uranium removal by *C. metallidurans* NA4U. Concentration of uranium in the supernatant (a) and total counts (b) after growth of NA4U without uranium (blue), in the presence of 100 μM (green) and 250 μM $UO_2(NO_3)_2$ (red) with (dark) and without CCCP (light). Results of the growth medium without cells are presented in brown. Values represent the average and standard deviation of three biological replicates.

4. Discussion

The β-proteobacterium *C. metallidurans* harbors a wide plethora of metal resistance gene clusters and is typically found in metal-contaminated environments (Mergeay and Van Houdt, 2015). It has become a model organism to study metal resistance and applications for biosensing and bioremediation of metals have been developed (Corbisier et al., 1999; Diels et al., 1999, 2009; Tibazarwa et al., 2001). Bioremediation is considered one of the most promising bio-based approaches for the remediation of uranium-contaminated sites (Newsome et al., 2014). The use of multiple-metal resistant bacteria would be an advantage as uranium contaminated soils are very often co-contaminated with metals such as cadmium, zinc and copper (Li and Krumholz, 2009; Bigalke et al., 2017; Lu and Liu, 2018). However, detailed knowledge on the interaction of *C. metallidurans* with uranium is lacking. In this study, we showed that *C. metallidurans* NA4 is able to adapt to toxic uranium concentrations. The obtained spontaneous mutant NA4U exhibited an active uranium accumulation mechanism by forming uranium-phosphate precipitates, similar as the parental strain (Rogiers et al., 2022a). Notably, the uranium resistant mutant harbored a second mechanism to cope with higher uranium concentrations, probably by relocating the uranium-phosphate precipitates to its periplasm. In general, uranium-phosphate precipitation is a known resistance mechanism for bacteria towards uranium but localization of the precipitates can be strain specific or even dependent on the pH or

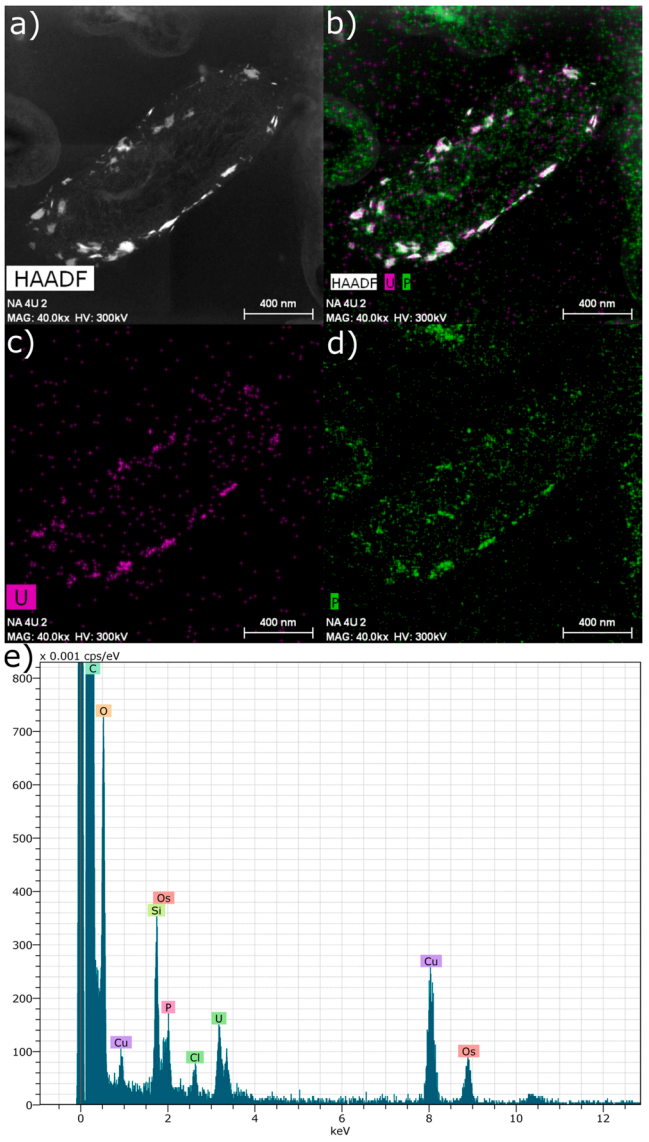

Fig. 5. Electron microscopy images of *C. metallidurans* NA4U in the presence of uranium. a) HAADF-STEM micrograph together with distribution analysis of b) uranium (purple) and phosphorus (green), c) uranium and d) phosphorus of *C. metallidurans* NA4U grown 24 h in presence of 250 μM $UO_2(NO_3)_2$. e) EDX spectra of a uranium structure at the cell membrane. The characteristic peaks of copper in the EDX spectra are caused by fluorescence excitation of the TEM support grid.

incubation time. For example, membrane-associated precipitates were found in *Caulobacter crescentus* NA1000 at circumneutral pH or for *Myxococcus xanthus* at pH 4.5, but uranium-phosphate complexes were also observed in the bulk medium (Jroundi et al., 2007; Yung and Jiao, 2014). *Serratia* sp. strain OT II 7 formed extracellular precipitates at pH 7 and pH 9. In contrast, uranium-phosphate was associated with the outer membrane after 10 h incubation at pH 5 but moved intracellularly at later time points (Chandwadkar et al., 2018). Membrane associated uranium accumulation was observed in *Bacillus sphaericus* JG-7B while both membrane associated and intracellular accumulation was observed in *Sphingomonas* sp. S15-S1 for a single concentration of $UO_2(NO_3)_2$ (Merroun et al., 2011). Our results show that localization of uranium-phosphate precipitates within a single strain can also depend on uranium concentrations.

Whole genome and transcriptome sequencing and insertional mutation revealed a role for the two-component system $CzcR_2S_2$ and a small periplasmic protein $PrsQ_2$ in the formation of the periplasmic precipitates. Deletion of *czcS*$_2$ resulted in transcriptional activation of the corresponding response regulator $CzcR_2$, which on its turn cross-activated the expression of the non-canonical target *prsQ*$_2$, resulting in the increased uranium resistance. A uranium responsive TCS system UzcRS was identified in *Caulobacter crescentus* and upstream the recently identified uranium binding protein UipA of *Microbacterium*, a TCS system UipRS is located (Park et al., 2017; Gallois et al., 2021). However, insertional mutants refuted a role for UzcRS in uranium resistance (Park et al., 2017). Moreover, the role of UipRS in uranium resistance is also unclear as the TCS is absent or not induced at proteomic level in uranium tolerant UipA positive strains (Gallois et al., 2021). In fact, no TCS system or regulator involved in uranium resistance was identified to date.

Notably, our observations are strikingly similar to the adaptive silver resistance mechanism observed in *C. metallidurans* NA4 (Mijnendonckx et al., 2019). Here, a mutation in the TCS AgrRS resulted in an increased resistance to silver without the involvement of the canonical silver resistant mechanisms. Rather, the unphosphorylated response regulator AgrR activated non-cognate targets, including *prsQ*$_2$ enabling the strain to withstand much higher silver concentrations (Mijnendonckx et al., 2019; Ali et al., 2020). $PrsQ_2$ is a member of an uncharacterized protein family of secreted intrinsically disordered proteins, whose members are restricted to the genera *Cupriavidus* and *Ralstonia* (Janssen et al., 2010; Mijnendonckx et al., 2019). Although their precise mode of action is not yet resolved, it seems that they are key proteins in adaptive resistance to metals including uranium and silver. The 62-AA long protein harbors 8 threonine and 3 serine residues, which are possible phosphorylation sites. Putatively, these residues play an important role in the formation of the periplasmic uranium phosphate precipitates. A different affinity for uranium explained by a distinct C-terminal region containing significantly more serine and threonine residues was also observed in an S-layer protein of *Bacillus sphaericus* where the SlfB S-layer protein of *B. sphaericus* JG-A12, isolated from a uranium mining waste pile expressing is much more effective in uranium binding than the SlfA S-layer protein of the reference strain *B. sphaericus* NCTC 9602 (Pollmann et al., 2005).

5. Conclusion

We showed that a single mutation in a sensor kinase increased the resistance of *C. metallidurans* NA4 to uranium four times. The increased uranium resistance was acquired via the formation of periplasmic uranium-phosphate precipitates facilitated by the increased expression of a genus-specific small periplasmic protein, $PrsQ_2$, regulated as non-cognate target of the $CzcS_2$-$CzcR_2$ two-component system. A more detailed study of members of this protein family can benefit the search of novel biological routes for metal remediation.

Environmental implication

Cupriavidus metallidurans is a model bacterium to study molecular mechanisms of metal resistance and its application as bioreporter for and in bioremediation of several metals has been shown. However, its molecular response towards radionuclides, which are often found in metal-contaminated environments, remains largely unexplored. We showed that a single mutation increased uranium resistance of strain *C. metallidurans* NA4 four times. The mutation resulted in the activation of a small periplasmic protein, which played a central role in the adaptation process by relocating uranium-phosphate precipitates in the periplasm. Understanding the detailed molecular resistance mechanisms can aid in exploiting bioremediation techniques.

CRediT authorship contribution statement

Kristel Mijnendonckx: Conceptualization, Design, Methodology, Supervision, Writing – original draft preparation **Tom Rogiers:** Conceptualization, Design, Methodology, Experimental work, Writing – original draft preparation. **Francisco J. Giménez del Rey:** Experimental work. **Mohamed L. Merroun**: Electron microscopy analysis. **Adam Williamson:** Methodology, **Md Muntasir Ali**: Experimental work. **Daniel Charlier:** Experimental work. **Natalie Leys:** Project resources **Nico Boon:** Project resources. **Rob Van Houdt:** Conceptualization, Design, Writing – reviewing and editing. All authors contributed to manuscript revision, read and approved the submitted version.

Declaration of Competing Interest

The authors declare that they have no known competing financial interests or personal relationships that could have appeared to influence the work reported in this paper.

Data availability

Datasets included in this study are included in the article or accessible online via the NCBI Sequence Read Archive (SRA) repository under accession number PRJNA849803.

Acknowledgements

We thank Gaurav Sharma for assistance with $CzcR_2$ cloning, expression and purification.

Appendix A. Supporting information

Supplementary data associated with this article can be found in the online version at doi:10.1016/j.jhazmat.2022.130410.

References

Ali, M.M., Provoost, A., Mijnendonckx, K., Van Houdt, R., Charlier, D., 2020. DNA-binding and transcription activation by unphosphorylated response regulator AgrR from cupriavidus metallidurans involved in silver resistance, 1635-1635 Front. Microbiol. 11. https://doi.org/10.3389/fmicb.2020.01635.

Ali, M.M., Provoost, A., Maertens, L., Leys, N., Monsieurs, P., Charlier, D., et al., 2019. Genomic and transcriptomic changes that mediate increased platinum resistance in cupriavidus metallidurans. Genes 10 (1). https://doi.org/10.3390/genes10010063.

Beazley, M.J., Martinez, R.J., Sobecky, P.A., Webb, S.M., Taillefert, M., 2007. Uranium biomineralization as a result of bacterial phosphatase activity: Insights from bacterial isolates from a contaminated subsurface. Environ. Sci. Technol. 41, 5701–5707. https://doi.org/10.1021/es070567g.

Bigalke, M., Ulrich, A., Rehmus, A., Keller, A., 2017. Accumulation of cadmium and uranium in arable soils in Switzerland. Environ. Pollut. 221, 85–93. https://doi.org/10.1016/j.envpol.2016.11.035.

Bobe, L., Kochetkov, A., Soloukhin, V., Ancreichuk, P., Protasov, N., and Sinyak, Y. (2008). "SRV-K Status Aboard the International Space Station during Missions 15 and 16", in: International Conference On Environmental Systems. (San Fransisco, CA, USA: SAE International).

Chandwadkar, P., Misra, H.S., Acharya, C., 2018. Uranium biomineralization induced by a metal tolerant Serratia strain under acid, alkaline and irradiated conditions. Metallomics 10 (8), 1078–1088. https://doi.org/10.1039/c8mt00061a.

Cologgi, D.L., Lampa-Pastirk, S., Speers, A.M., Kelly, S.D., Reguera, G., 2011. Extracellular reduction of uranium via Geobacter conductive pili as a protective cellular mechanism. PNAS 108 (37), 15248–15252. https://doi.org/10.1073/pnas.1108616108.

Corbisier, P., van der Lelie, D., Borremans, B., Provoost, A., de Lorenzo, V., Brown, N.L., et al., 1999. Whole cell- and protein-based biosensors for the detection of bioavailable heavy metals in environmental samples. Anal. Chim. Acta 387 (3), 235–244. https://doi.org/10.1016/S0003-2670(98)00725-9.

Diels, L., De Smet, M., Hooyberghs, L., Corbisier, P., 1999. Heavy metals bioremediation of soil. Mol. Biotechnol. 12 (2), 149–158. https://doi.org/10.1385/MB:12:2:149.

Diels, L., Van Roy, S., Taghavi, S., Van Houdt, R., 2009. From industrial sites to environmental applications with Cupriavidus metallidurans. Antonie Van. Leeuwenhoek 96 (2), 247–258. https://doi.org/10.1007/s10482-009-9361-4.

Diels, L., Dong, Q., van der Lelie, D., Baeyens, W., Mergeay, M., 1995. The czc operon of Alcaligenes eutrophus CH34: from resistance mechanism to the removal of heavy metals. J. Ind. Microbiol 14 (2), 142–153. https://doi.org/10.1007/bf01569896.

Enoru-Eta, J., Gigot, D., Thia-Toong, T.L., Glansdorff, N., Charlier, D., 2000. Purification and characterization of Sa-lrp, a DNA-binding protein from the extreme thermoacidophilic archaeon Sulfolobus acidocaldarius homologous to the bacterial global transcriptional regulator Lrp. J. Bacteriol. 182 (13), 3661–3672. https://doi.org/10.1128/jb.182.13.3661-3672.2000.

Ferrieres, L., Hemery, G., Nham, T., Guerout, A.M., Mazel, D., Beloin, C., et al., 2010. Silent mischief: bacteriophage Mu insertions contaminate products of Escherichia coli random mutagenesis performed using suicidal transposon delivery plasmids mobilized by broad-host-range RP4 conjugative machinery. J. Bacteriol. 192 (24), 6418–6427. https://doi.org/10.1128/JB.00621-10.

Gallois, N., Alpha-Bazin, B., Bremond, N., Ortet, P., Barakat, M., Piette, L., et al., 2021. Discovery and characterization of UipA, a uranium- and iron-binding PepSY protein involved in uranium tolerance by soil bacteria. ISME J. https://doi.org/10.1038/s41396-021-01113-7.

Heath, B.S., Marshall, M.J., Laskin, J., 2014. Identification of mutations in laboratory evolved microbes from next-generation sequencing data using breseq. Methods Mol. Biol. 1151, 165–168. https://doi.org/10.1007/978-1-4939-0554-6_12.

IAEA, 2003. Extent of Environmental contamination by naturally occurring radioactive material (NORM) and technological options for mitigation. IAEA Rep. 419, 419.

IAEA (2018). The Fukushima Daiichi Accident. doi: 10.1037/a0018137.

Ikonomidis, A., Tsakris, A., Kanellopoulou, M., Maniatis, A.N., Pournaras, S., 2008. Effect of the proton motive force inhibitor carbonyl cyanide-m-chlorophenylhydrazone (CCCP) on Pseudomonas aeruginosa biofilm development. Lett. Appl. Microbiol. 47 (4), 298–302. https://doi.org/10.1111/j.1472-765x.2008.02430.x.

Janssen, P.J., Van Houdt, R., Moors, H., Monsieurs, P., Morin, N., Michaux, A., et al., 2010. The complete genome sequence of Cupriavidus metallidurans strain CH34, a master survivalist in harsh and anthropogenic environments. PLoS One 5 (5), e10433. https://doi.org/10.1371/journal.pone.0010433.

Jroundi, F., Merroun, M.L., Arias, J.M., Rossberg, A., Selenska-Pobell, S., González-Muñoz, M.T., 2007. Spectroscopic and microscopic characterization of uranium biomineralization in Myxococcus xanthus. Geomicrobiol. J. 24 (5), 441–449. https://doi.org/10.1080/01490450701437651.

Khare, D., Kumar, R., Acharya, C., 2020. Genomic and functional insights into the adaptation and survival of Chryseobacterium sp. strain PMSZPI in uranium enriched environment. Ecotoxicol. Environ. Saf. 191 (January), 110217 https://doi.org/10.1016/j.ecoenv.2020.110217.

Kovach, M.E., Elzer, P.H., Steven Hill, D., Robertson, G.T., Farris, M.A., Roop, R.M., et al., 1995. Four new derivatives of the broad-host-range cloning vector pBBR1MCS, carrying different antibiotic-resistance cassettes. Gene 166 (1), 175–176. https://doi.org/10.1016/0378-1119(95)00584-1.

Kulkarni, S., Ballal, A., Apte, S.K., 2013. Bioprecipitation of uranium from alkaline waste solutions using recombinant *Deinococcus radiodurans*. J. Hazard. Mater 262, 853–861. https://doi.org/10.1016/j.jhazmat.2013.09.057.

Li, X., Krumholz, L.R., 2009. Thioredoxin is involved in U(VI) and Cr(VI) reduction in Desulfovibrio desulfuricans G20. J. Bacteriol. 191 (15), 4924–4933. https://doi.org/10.1128/JB.00197-09.

Liao, Y., Smyth, G.K., Shi, W., 2019. The R package Rsubread is easier, faster, cheaper and better for alignment and quantification of RNA sequencing reads. Nucleic Acids Res. 47 https://doi.org/10.1093/nar/gkz114.

Llorens, I., Untereiner, G., Jaillard, D., Gouget, B., Chapon, V., Carriere, M., 2012. Uranium interaction with two multi-resistant environmental bacteria: cupriavidus metallidurans CH34 and rhodopseudomonas palustris. Plos One 7 (12). https://doi.org/10.1371/journal.pone.0051783.

Lu, Z., Liu, Z., 2018. Pollution characteristics and risk assessment of uranium and heavy metals of agricultural soil around the uranium tailing reservoir in Southern China. J. Radioanal. Nucl. Chem. 318 (2), 923–933. https://doi.org/10.1007/s10967-018-6081-0.

Ma, M., Wang, R., Xu, L., Xu, M., Liu, S., 2020. Emerging health risks and underlying toxicological mechanisms of uranium contamination: Lessons from the past two decades. Environ. Int. 145, 106107 https://doi.org/10.1016/j.envint.2020.106107.

Macaskie, L.E., Bonthrone, K.M., Yong, P., Goddard, D.T., 2000. Enzymically mediated bioprecipitation of uranium by a *Citrobacter* sp.: A concerted role for exocellular lipopolysaccharide and associated phosphatase in biomineral formation. Microbiology 146, 1855–1867. https://doi.org/10.1099/00221287-146-8-1855.

Mergeay, M., Van Houdt, R. (Eds.), 2015. Metal response in *Cupriavidus metallidurans*. Volume I, From habitats to genes and proteins. Springer Cham.

Mergeay, M., Nies, D., Schlegel, H.G., Gerits, J., Charles, P., Van Gijsegem, F., 1985. Alcaligenes eutrophus CH34 is a facultative chemolithotroph with plasmid-bound resistance to heavy metals. J. Bacteriol. 162 (1), 328–334.

Merroun, M.L., Nedelkova, M., Ojeda, J.J., Reitz, T., Fernández, M.L., Arias, J.M., et al., 2011. Bio-precipitation of uranium by two bacterial isolates recovered from extreme environments as estimated by potentiometric titration, TEM and X-ray absorption spectroscopic analyses. J. Hazard. Mater. 197, 1–10. https://doi.org/10.1016/j.jhazmat.2011.09.049.

Mijnendonckx, K., Provoost, A., Monsieurs, P., Leys, N., Mergeay, M., Mahillon, J., et al., 2011. Insertion sequence elements in Cupriavidus metallidurans CH34: Distribution and role in adaptation. S0147-619X(10)00115-0 [pii] Plasmid 65 (3), 193–203. https://doi.org/10.1016/j.plasmid.2010.12.006.

Mijnendonckx, K., Ali, M.M., Provoost, A., Janssen, P., Mergeay, M., Leys, N., et al., 2019. Spontaneous mutation in the AgrRS two-component regulatory system of Cupriavidus metallidurans results in enhanced silver resistance. Metallomics. https://doi.org/10.1039/c9mt00123a.

Newsome, L., Morris, K., Lloyd, J.R., 2014. The biogeochemistry and bioremediation of uranium and other priority radionuclides. Chem. Geol. 363, 164–184. https://doi.org/10.1016/j.chemgeo.2013.10.034.

Nguyen Ple, M., Bervoets, I., Maes, D., Charlier, D., 2010. The protein-DNA contacts in RutR*carAB operator complexes. Nucleic Acids Res 38 (18), 6286–6300. https://doi.org/10.1093/nar/gkq385.

Nies, D., Mergeay, M., Friedrich, B., Schlegel, H.G., 1987. Cloning of plasmid genes encoding resistance to cadmium, zinc, and cobalt in Alcaligenes eutrophus CH34. J. Bacteriol. 169 (10), 4865–4868.

Nilgiriwala, K.S., Alahari, A., Rao, A.S., Apte, S.K., 2008. Cloning and overexpression of alkaline phosphatase PhoK from *Sphingomonas* sp. strain BSAR-1 for bioprecipitation of uranium from alkaline solutions. Appl. Environ. Microbiol 74, 5516–5523. https://doi.org/10.1128/AEM.00107-08.

Park, D.M., Overton, K.W., Liou, M.J., Jiao, Y., 2017. Identification of a U/Zn/Cu responsive global regulatory two-component system in Caulobacter crescentus. Mol. Microbiol. 104 (1), 46–64. https://doi.org/10.1111/mmi.13615.

Pinel-Cabello, M., Jroundi, F., López-Fernández, M., Geffers, R., Jarek, M., Jauregui, R., et al., 2021. Multisystem combined uranium resistance mechanisms and bioremediation potential of Stenotrophomonas bentonitica BII-R7: Transcriptomics and microscopic study. J. Hazard. Mater. 403. https://doi.org/10.1016/j.jhazmat.2020.123858.

Pollmann, K., Raff, J., Schnorpfeil, M., Radeva, G., Selenska-Pobell, S., 2005. Novel surface layer protein genes in Bacillus sphaericus associated with unusual insertion elements. Microbiology 151 (9), 2961–2973. https://doi.org/10.1099/mic.0.28201-0.

Powell, S., Szklarczyk, D., Trachana, K., Roth, A., Kuhn, M., Muller, J., Arnold, R., Rattei, T., Letunic, I., Doerks, T., Jensen, L.J., Von Mering, C., Bork, P., 2012. eggNOG v3.0: Orthologous groups covering 1133 organisms at 41 different taxonomic ranges. Nucleic Acids Res. 40, 284–289. https://doi.org/10.1093/nar/gkr1060.

Powers, L.G., Mills, H.J., Palumbo, A.V., Zhang, C., Delaney, K., Sobecky, P.A., 2002. Introduction of a plasmid-encoded *phoA* gene for constitutive overproduction of alkaline phosphatase in three subsurface *Pseudomonas* isolates. FEMS Microbiol. Ecol 41, 115–123. https://doi.org/10.1016/S0168-6496(02)00263-5.

R Core Team (2017). R: A Language and Environment for Statistical Computing [Online]. Vienna, Austria: R Foundation for Statistical Computing. Available: ⟨https://www.R-project.org/⟩ [Accessed].

Raghavan, N., Verbeke, T., De Bondt, A., Cabrera, J., Amaratunga, D., Casneuf, T., Ligtenberg, W.. MLP: MLP. R package version 1.34.0. https://www.bioconductor.org/packages/release/bioc/html/MLP.html.

Rajkumar, M., Ae, N., Prasad, M.N.V., Freitas, H., 2010. Potential of siderophore-producing bacteria for improving heavy metal phytoextraction. Trends Biotechnol. 28 (3), 142–149. https://doi.org/10.1016/j.tibtech.2009.12.002.

Ritchie, M.E., Phipson, B., Wu, D., Hu, Y., Law, C.W., Shi, W., Smyth, G.K., 2015. Limma powers differential expression analyses for RNA-sequencing and microarray studies. Nucleic Acids Res. 43 https://doi.org/10.1093/nar/gkv007.

Robinson, M.D., McCarthy, D.J., Smyth, G.K., 2009. edgeR: A Bioconductor package for differential expression analysis of digital gene expression data. Bioinformatics 43, 139–140. https://doi.org/10.1093/bioinformatics/btp616.

Rogiers, T., 2022. Uranium resistance mechanisms in Cupriavidus metallidurans: from environmental relevance to potential applications (PhD). Ghent University,.

Rogiers, T., Merroun, M.L., Williamson, A., Leys, N., Houdt, R.V., Boon, N., et al., 2022a. Cupriavidus metallidurans NA4 actively forms polyhydroxybutyrate-associated uranium-phosphate precipitates. J. Hazard Mater. 421, 126737 https://doi.org/10.1016/j.jhazmat.2021.126737.

Rogiers, T., Van Houdt, R., Williamson, A., Leys, N., Boon, N., Mijnendonckx, K., 2022b. Molecular mechanisms underlying bacterial uranium resistance. Front. Microbiol. 13. https://doi.org/10.3389/fmicb.2022.822197.

Schafer, A., Tauch, A., Jager, W., Kalinowski, J., Thierbach, G., Puhler, A., 1994. Small mobilizable multi-purpose cloning vectors derived from the Escherichia coli plasmids pK18 and pK19: selection of defined deletions in the chromosome of Corynebacterium glutamicum. Gene 145 (1), 69–73.

Simonoff, M., Sergeant, C., Poulain, S., Pravikoff, M.S., 2007. Microorganisms and migration of radionuclides in environment. Comptes Rendus Chim. 10 (10–11), 1092–1107. https://doi.org/10.1016/j.crci.2007.02.010.

Smith, D.K., Finnegan, D.L., Bowen, S.M., 2003. An inventory of long-lived radionuclides residual from underground nuclear testing at the Nevada test site, 1951–1992. J. Environ. Radioact. 67 (1), 35–51. https://doi.org/10.1016/S0265-931X(02)00146-7.

Sprouffske, K., Wagner, A., 2016. Growthcurver: an R package for obtaining interpretable metrics from microbial growth curves. BMC Bioinforma. 17 (1), 172. https://doi.org/10.1186/s12859-016-1016-7.

Theodorakopoulos, N., Chapon, V., Coppin, F., Floriani, M., Vercouter, T., Sergeant, C., et al., 2015. Use of combined microscopic and spectroscopic techniques to reveal interactions between uranium and Microbacterium sp. A9, a strain isolated from the Chernobyl exclusion zone. J. Hazard. Mater. 285, 285–293. https://doi.org/10.1016/j.jhazmat.2014.12.018.

Tibazarwa, C., Corbisier, P., Mench, M., Bossus, A., Solda, P., Mergeay, M., et al., 2001. A microbial biosensor to predict bioavailable nickel in soil and its transfer to plants (Doi). Environ. Pollut. 113 (1), 19–26. https://doi.org/10.1016/S0269-7491(00)00177-9.

Unscear (1988). "Report to the general assembly (Annex D— Exposures from Chernobyl accident).").

Vallenet, D., Belda, E., Calteau, A., Cruvellier, S., Engelen, S., Lajus, A., Le Févre, F., Longin, C., Mornico, D., Roche, D., et al., 2013. MicroScope - An integrated microbial resource for the curation and comparative analysis of genomic and metabolic data. Nucleic Acids Res. 41, 636–647. https://doi.org/10.1093/nar/gks1194.

Van Houdt, R., Provoost, A., Van Assche, A., Leys, N., Lievens, B., Mijnendonckx, K., et al., 2018. Cupriavidus metallidurans Strains with Different Mobilomes and from Distinct Environments Have Comparable Phenomes. Genes 9 (10). https://doi.org/10.3390/genes9100507.

You, W., Peng, W., Tian, Z., Zheng, M., 2021. Uranium bioremediation with U(VI)-reducing bacteria. Sci. Total Environ. 798, 149107 https://doi.org/10.1016/j.scitotenv.2021.149107.

Yu, Q., Yuan, Y., Feng, L., Sun, W., Lin, K., Zhang, J., et al., 2022. Highly efficient immobilization of environmental uranium contamination with Pseudomonas stutzeri by biosorption, biomineralization, and bioreduction. J. Hazard. Mater. 424, 127758 https://doi.org/10.1016/j.jhazmat.2021.127758.

Yun, J., Malvankar, N.S., Ueki, T., Lovley, D.R., 2016. Functional environmental proteomics: elucidating the role of a c-type cytochrome abundant during uranium bioremediation. ISME J. 10 (2), 310–320. https://doi.org/10.1038/ismej.2015.113.

Yung, M.C., Jiao, Y., 2014. Biomineralization of uranium by PhoY phosphatase activity aids cell survival in *Caulobacter crescentus*. Appl. Environ. Microbiol. 80 (16), 4795–4804. https://doi.org/10.1128/AEM.01050-14.

Yung, M.C., Park, D.M., Overton, K.W., Blow, M.J., Hoover, C.A., Smit, J., et al., 2015. Transposon mutagenesis paired with deep sequencing of caulobacter crescentus under uranium stress reveals genes essential for detoxification and stress tolerance. J. Bacteriol. 197 (19), 3160–3172. https://doi.org/10.1128/jb.00382-15.